

Interpretation of the cosmic ray positron and antiproton fluxes

Paolo Lipari^{1,*}

¹*INFN sezione Roma "Sapienza"*

The spectral shape of cosmic ray positrons and antiprotons has been accurately measured in the broad kinetic energy range 1–350 GeV. In the higher part of this range ($E \gtrsim 30$ GeV) the e^+ and \bar{p} are both well described by power laws with spectral indices $\gamma_{e^+} \simeq 2.77 \pm 0.02$ and $\gamma_{\bar{p}} \simeq 2.78 \pm 0.04$ that are approximately equal to each other and to the spectral index of protons. In the same energy range the positron/antiproton flux ratio has the approximately constant value 2.04 ± 0.04 , that is consistent with being equal to the ratio e^+/\bar{p} calculated for the conventional mechanism of production, where the antiparticles are created as secondaries in the inelastic interactions of primary cosmic rays with interstellar gas. The positron/antiproton ratio at lower energy is significantly higher (reaching a value $e^+/\bar{p} \approx 100$ for $E \approx 1$ GeV), but in the entire energy range 1–350 GeV, the flux ratio is consistent with being equal to ratio of the production rates in the conventional mechanism, as the production of low energy antiprotons is kinematically suppressed in collisions with a target at rest. These results strongly suggest that cosmic ray positrons and antiprotons have a common origin as secondaries in hadronic interactions. This conclusion has broad implications for the astrophysics of cosmic rays in the Galaxy.

arXiv:1608.02018v1 [astro-ph.HE] 5 Aug 2016

*Electronic address: paolo.lipari@roma1.infn.it

I. INTRODUCTION

The study of cosmic ray positrons and antiprotons is a very important topic in high energy astrophysics and has received a very large amount of attention in recent years. A strong motivation for these studies is the possibility that, if the Galactic Dark Matter (DM) is in the form of Weakly Interacting Massive Particles (WIMP's), the self-annihilation or decay of the DM particles can be an observable source of relativistic antiparticles.

The only known mechanism that can generate a detectable flux of high energy positrons and antiprotons in the Galaxy is their production as secondaries in the inelastic interactions of primary cosmic rays (CR) in interstellar space, or perhaps inside or around the astrophysical sites where CR are accelerated. This conventional mechanism has to be well understood to establish the existence of other contributions generated by alternative mechanisms (such as DM annihilation, or direct acceleration in some classes of astrophysical sources).

The study of the CR fluxes of antiparticles has made a very important step forward thanks to the measurements performed by PAMELA of positrons [1, 2] and anti-protons [3]. The PAMELA observation showed that the positron flux, for $E \gtrsim 10$ GeV, is significantly harder than predictions based on the conventional mechanism, and this discrepancy has generated an intense attention and a large body of literature.

The PAMELA results for the positron flux have been confirmed by observations of the FERMI detector [4] performed using the Earth magnetic field to separate the fluxes of CR electrons and positrons. More recently the AMS02 detector, on the International Space Station has measured the e^+ spectrum [5], in good agreement with PAMELA, and with smaller errors and extending the observations up to an energy $E \simeq 400$ GeV.

Most of the literature that discusses the CR positron flux takes the point of view that the observations require a new, non-standard source of positrons. Only few works have taken the point of view that the discrepancy between predictions and observations must be attributed to an incorrect estimate of the positron flux generated by the conventional (secondary production) mechanism.

In contrast to the situation for positrons, the measurements of antiprotons performed by PAMELA are consistent with the predictions based on the conventional mechanism of production. This is clearly a very important constraint for the interpretation of the antiparticle data, because many sources of e^+ are also sources of \bar{p} (and vice-versa). The comparison of positron and antiproton fluxes is therefore crucial to determine the nature and properties of the physical mechanisms that generate antiparticles in the Galaxy.

Recently, the AMS02 collaboration has presented new preliminary results [6] on the \bar{p}/p ratio. These results are in very good agreement with the PAMELA measurements, but have smaller errors and extend to higher energy (up to $E \simeq 350$ GeV). This allows to determine the shape of the antiproton spectrum with much greater precision.

Having in hands precision measurements of the positron and antiproton fluxes that extend in a broad energy range, together with high quality measurements of the spectra of primary CR particles (protons, electrons and nuclei) allows to perform detailed comparisons that can give important insight about the origin of the different CR components. This work is dedicated to a critical discussion of some intriguing results that emerge from these comparisons.

For energies larger than approximately 30 GeV the spectra of protons, electrons, antiprotons and positrons are well described by power laws ($\phi_j(E) \propto E^{-\gamma_j}$). It is remarkable that the spectral indices for positrons and antiprotons are consistent with being equal ($\gamma_{e^+} \simeq 2.77 \pm 0.02$ and $\gamma_{\bar{p}} \simeq 2.78 \pm 0.04$), and are also very close to the spectral index for protons. Only the electron flux has a different shape, and is much softer with a larger spectral index of order $\gamma_{e^-} \approx 3.2$.

The e^+/\bar{p} ratio is approximately constant in the energy range [30–350] GeV with value 2.04 ± 0.04 . This value is also equal (taking into account systematic uncertainties) to the e^+/\bar{p} ratio *at production* for the conventional mechanism. In fact it is possible to show the numerical validity of a stronger result: the observed e^+/\bar{p} ratio, is consistent with being equal to the ratio e^+/\bar{p} calculated for the conventional mechanism of secondary production, in the entire energy range [1–350] GeV, including the lower energy part where the positron/antiproton ratio changes rapidly with E , taking the value $e^+/\bar{p} \approx 100$ for kinetic energy $E \approx 1$ GeV.

These intriguing results, are perhaps just a numerical accident but, at least at face value, seem to indicate that the CR fluxes of both positrons and antiprotons have their origin in the conventional secondary production mechanism. This is in contrast to all models where e^+ and \bar{p} have different origin. This interpretation has however some non trivial difficulties, and requires a deep revision of some important concepts for the formation and propagation of the Galactic cosmic rays. In the following we will attempt to discuss critically these problems.

This work is organized as follows. The next section summarizes recent measurements of the cosmic ray fluxes. Section III discusses the production of positrons and antiprotons in hadronic interactions, and computes the antiparticles production rates in the solar neighborhood. Section IV discusses the energy losses of relativistic particles propagating in the Galaxy. Section V outlines some general concepts about the formation of the CR fluxes in the Galaxy, and describes what can be considered the current (broadly, but not universally accepted) “standard framework” for the study of the Galactic Cosmic Rays. Section VI discusses alternative frameworks for CR in the Galaxy that can explain naturally the correlations between the positron and antiproton fluxes. The final section gives a summary

and comments of the most promising directions for future studies to clarify the situation. The appendix A discusses an analytic estimate for the ratio e^+/\bar{p} at production under the assumption that the antiparticles are generated as secondaries in inelastic hadronic interactions.

II. COSMIC RAY FLUXES

Recent measurements of the fluxes of protons, electrons, antiprotons and positrons are shown in Fig. 1 in the form $\phi_j(E) \times E^{2.7}$ versus E (with E the kinetic energy) to enhance the visualization of spectral features. Note that the proton flux is rescaled by a factor 10^{-2} .

The measurements are by PAMELA (for p , \bar{p} and e^\mp) [2, 3, 7, 8], AMS02 (also p , \bar{p} and e^\mp) [5, 6, 9], CREAM (p at high energy) [10], FERMI ($e^+ + e^-$) [11] and HESS ($e^+ + e^-$) [12, 13].

The AMS results of antiprotons are preliminary and have been presented in the form of the ratio \bar{p}/p as a function of rigidity. We have read these results graphically from the slides available in [6] and transformed the ratio into an absolute flux, using a smooth fit (also shown in the figure) to the proton flux measurements performed by the same experiment, and changed variable from rigidity to kinetic energy. The measurements of the e^+ and \bar{p} spectra are also shown with an enlarged scale in Fig. 2.

Inspecting the figures one can make the following remarks:

- The proton flux for $E \gtrsim 30$ GeV has approximately a power law form ($\phi_p(E) \propto E^{-\gamma_p}$) with an intriguing hardening feature at energy $E \simeq 300$ GeV. The feature was first deduced by CREAM [14], then directly observed by PAMELA [8] and now is also clearly confirmed by the AMS02 data [9]. The AMS02 collaboration [9] has fitted its measurement of the proton flux as the transition between two power laws with exponents γ_p and $\gamma_p + \Delta\gamma_p$ above and below the transition momentum $p^* \simeq 336_{-26}^{+44}$ GeV. The best fit values of the parameters are: $\gamma_p \simeq 2.849_{-0.005}^{+0.006}$ and $\Delta\gamma_p = -0.133_{-0.037}^{+0.056}$.
- The electron flux is smaller and significantly softer than the proton flux. The ratio e^-/p of the electron and proton fluxes is shown in Fig. 3. For low kinetic energy ($0.5 \lesssim E \lesssim 2$ GeV) the ratio e^-/p has a value of order 0.03. Increasing E the ratio falls rapidly, and at $E = 100$ GeV it is approximately 3×10^{-3} , one order of magnitude smaller. The energy dependence of the ratio in the energy range $E \in [30, 300]$ GeV is reasonably well described by a power law:

$$\left. \frac{\phi_{e^-}(E)}{\phi_p(E)} \right|_{E \in [30, 300] \text{ GeV}} \simeq (3.95 \pm 0.10) \times 10^{-3} \left(\frac{E}{50 \text{ GeV}} \right)^{-0.41 \pm 0.02} \quad (1)$$

- Inspecting Fig. 1 and 2 it is apparent that for kinetic energy $E \gtrsim 20$ –30 GeV the spectra of positrons and antiprotons have a shape that is reasonably well approximated by a simple power law. To test this hypothesis, we have fitted the AMS02 data points in the energy range $E > 30$ GeV with the functional form:

$$\phi_j(E) = K_j \left(\frac{E}{50 \text{ GeV}} \right)^{-\gamma_j} \quad (2)$$

(with $j = e^+$ or \bar{p}). For positrons we obtain a best fit with $\chi_{\min}^2 = 12.0$ for 27 degrees of freedom (d.o.f.), and best fit parameters $K_{e^+} = (11.4 \pm 0.1) \times 10^{-5} \text{ (m}^2\text{sr GeV)}^{-1}$ and $\gamma_{e^+} = 2.77 \pm 0.02$. The χ^2 of the fit has been calculated summing in quadrature statistical and systematic errors, the resulting value of χ_{\min}^2 is small, indicating the existence of correlations in the systematic errors for different points. For antiprotons the best fit has $\chi_{\min}^2 = 1.56$ for 10 d.o.f. with best fit parameters $K_{\bar{p}} = (5.6 \pm 0.1) \times 10^{-5} \text{ (m}^2\text{sr GeV)}^{-1}$, and $\gamma_{\bar{p}} = 2.78 \pm 0.04$.

It is remarkable that the estimate of the (approximately constant) spectral indices of the positron and antiproton spectra in the energy range $E \in [30, 350]$ GeV are consistent with being equal. It is also intriguing that the spectral indices of the antiparticle fluxes are very close to the spectral index for protons:

$$\gamma_{e^+} \simeq \gamma_{\bar{p}} \approx \gamma_p + \frac{\Delta\gamma_p}{2} \quad (3)$$

In the following we will discuss if these results are a simple coincidence or have a deeper physical explanation.

- The positron/antiproton ratio can be estimated combining the results of the two fits:

$$\left. \frac{\phi_{e^+}(E)}{\phi_{\bar{p}}(E)} \right|_{E \in [30, 350] \text{ GeV}} \simeq (2.04 \pm 0.04) \times \left(\frac{E}{50 \text{ GeV}} \right)^{0.015 \pm 0.045} \quad (4)$$

that is consistent with a constant value. This result is in striking contrast with the behavior of the e^-/p ratio (given in equation (1)) that in the same energy range falls rapidly with energy.

The energy dependence of the e^+/\bar{p} ratio in a broader energy range is shown in Fig. 3. For low kinetic energy the ratio varies rapidly with E . At $E \simeq 1$ GeV it is of order 100, and decreases monotonically to reach the approximately constant value of order 2 at $E \simeq 20\text{--}30$ GeV.

- Measurements of the spectrum of the sum ($e^+ + e^-$) at very high energy have been obtained by the ground based Atmospheric Cherenkov telescopes HESS [12, 13], MAGIC [15] and VERITAS [16]. The results of three Cherenkov telescopes are shown in Fig. 4.

These results show the existence of a sharp softening of the ($e^+ + e^-$) spectrum at an energy just below 1 TeV. The HESS Collaboration has published a best fit to the data using a broken power with break at energy $E \simeq 900$ GeV, where the spectral index changes from $\gamma_1 \simeq 3.0$ to $\gamma_2 \simeq 4.1$ (no errors are reported). The VERITAS [16] has also performed a fit using the same broken power law functional form, finding the break at $E \simeq 710 \pm 40$ GeV and spectral indices $\gamma_1 \simeq 3.2 \pm 0.1$ and $\gamma_2 \simeq 4.1 \pm 0.1$ (all errors are only statistical). The origin of this very prominent feature remains controversial (see discussion in following).

III. HADRONIC INTERACTIONS AND THE PRODUCTION OF e^+ AND \bar{p}

The “normal” mechanism for the production of relativistic positrons and antiprotons is their creation as secondaries in the inelastic interactions of primary cosmic rays with some target material. The leading contribution to this production mechanism is due to pp interaction where one relativistic proton collides with a target proton at rest. Additional contributions are due to helium–proton, proton–helium, helium–helium, ... collisions, where different types of CR primary particles interact with different target nuclei. In inelastic hadronic collisions baryon/antibaryon pairs can be created, and after chain decay each antibaryon generates one stable antiproton that enters the CR population. The most abundant source of positrons in hadronic interactions is the creation and chain decay of π^+ :

$$\pi^+ \rightarrow \nu_\mu + \mu^+ \rightarrow \nu_\mu + [e^+ + \nu_e + \bar{\nu}_\mu] .$$

The spectrum of the positrons generated in this decay can be calculated exactly using the (non-trivial) matrix element for the 3-body muon decay, and taking into account the fact that the muons created in the first decay are in a well defined polarization state (see for example [17]). A subdominant, but not entirely negligible, source of positrons is the production and chain decay of kaons. Also in this case it is straightforward to compute the positron spectrum generated by the decay of a kaon, summing over all chain decay modes (weighted by the appropriate branching ratios). For example a K^+ can generate positrons either directly (in the decay mode $K^+ \rightarrow e^+ \nu_e \pi^0$) or after several chain decay modes (such as in $K^+ \rightarrow \mu^+ \nu_\mu \rightarrow e^+ \dots$).

The leading (pp) contribution to the local production rate (that is the number of particles created per unit time, unit volume and unit energy) of positrons (or antiprotons) can be written explicitly as:

$$q_{pp \rightarrow e^+(\bar{p})}^{\text{loc}}(E) = n_{\text{ism},p}(\vec{x}_\odot) \int_E^\infty dE_0 n_p^{\text{loc}}(E_0) \beta c \sigma_{pp}(E_0) \left[\frac{dN}{dE}(E, E_0) \right]_{pp \rightarrow e^+(\bar{p})} . \quad (5)$$

In this equation $n_{\text{ism},p}(\vec{x}_\odot)$ is the density of protons in interstellar gas in the solar neighborhood, $n_p^{\text{loc}}(E_0)$ is the number density of CR protons with energy E_0 in the vicinity of the Sun, βc is the proton velocity, $\sigma_{pp}(E_0)$ is the pp inelastic cross section (for collisions with a proton at rest), and $dN_{pp \rightarrow j}/dE$ is the inclusive spectrum of secondary particles of type j in the final state of the collision, calculated allowing the chain decay of all unstable parents. The density in interstellar space is so low that it is safe to assume that all unstable particles decay without suffering energy losses. The integration is over all possible energies of the interacting proton.

The other contributions to the production of e^+ and \bar{p} (such as p -helium or helium- p) can be obtained with obvious substitutions.

In the following we will show the results of a complete calculation of the local production rate of positrons and antiprotons, performed integrating numerically equation (5) and the other contributions. The calculation is straightforward and requires three basic elements:

- (i) An estimate of the density (and composition) of interstellar gas in the solar neighborhood.
- (ii) An estimate of the fluxes of CR protons and nuclei in the local interstellar medium.
- (iii) A model for the properties of inelastic hadronic interactions.

For the density of the interstellar gas we have used the value $n_{\text{ism}} = 1 \text{ cm}^{-3}$ and assumed a standard composition with a helium contribution of 9%.

The CR density in the local interstellar space can be easily related to the flux $\phi_j^{\text{loc}}(E)$ using the (very good) approximation of isotropy. For example for protons:

$$n_p^{\text{loc}}(E) = \frac{4\pi}{\beta c} \phi_p^{\text{loc}}(E) . \quad (6)$$

A more difficult step is the estimate of the local interstellar spectra from the CR measurements performed near the Earth deconvolving the effects of the (time dependent) solar modulations. The model of the cosmic ray fluxes used in this calculation is shown in figure 5 in the form of the all-nucleon flux versus the kinetic energy per nucleon. The model is based on fits to the AMS02 proton and helium data [9, 19] with a contribution of order 10% from heavier nuclei estimated from the data of the HEAO detector [21]. At higher energy it joins smoothly with the model of Gaisser, Stanev and Tilav [20].

To unfold the effects of solar modulations, we have assumed that the modulations is described by the Force Field Approximation (FFA) [22]. In the FFA the solar modulations depend on one (time dependent) parameter, the potential $V(t)$. The physical meaning of $V(t)$ is that particles with electric charge Z that penetrate the heliosphere and reach the Earth lose the energy $\Delta E = |Z|V(t)$. This is sufficient (using the Liouville theorem) to compute the observable flux at the Earth, and the algorithm can also be inverted analytically [23]. To take into account theoretical uncertainties we have calculated the CR spectra in the local interstellar space deconvolving the CR measurements shown in Fig. 5 with three values of the potential ($V = 0.4, 0.6$ and 0.9 GeV). This gives a non negligible range of uncertainty for primary energies $E \lesssim 50$ GeV. At higher energy the corrections associated to the solar modulations become negligible.

In order to compute the spectra of secondary positrons and antiprotons with an energy as large as $E \simeq 400$ GeV it is necessary to have a description of the primary fluxes up to an energy per nucleon of order 40 TeV. This requires an extrapolation of the measurements performed by the magnetic spectrometers, and requires a modeling of the hardening feature observed at a rigidity of order 250–300 GV. This is an important source of uncertainty.

The final element required for the calculation of the production rates of antiparticles is a model for the inclusive spectra of secondaries in inelastic hadronic interactions. This is probably the main source of systematic uncertainty in the calculation. For a calculation that covers the entire energy range $E \gtrsim 1$ GeV, we have used simple analytic descriptions of the differential cross sections for the production of secondary hadrons in pp interactions constructed on the basis of fixed target accelerator data. For \bar{p} production we have used the parametrization of Tan and Ng [24] assuming also that the interactions generate equal spectra of antiprotons and antineutrons. For the production of charged pions we used the parametrizations of Badhwar et al. [25], for kaons the work of Anticic et al. [26].

For a cross check, and to have a first order estimate of the size of the uncertainties we have also performed a calculation, using the Monte Carlo code Pythia (version 6.4) [27] to obtain numerically the spectra of secondaries. The Pythia code is reliable only at sufficiently high energy, and we have performed this calculation only for (positron and antiproton) energy $E \geq 100$ GeV.

The results of the calculation of the local production rates of e^+ and \bar{p} are shown in Fig. 6. plotted in the form $q_j(E) \times E^{2.7}$ versus the kinetic energy E . Some interesting features of the numerical results are listed below (in the following of this section we will drop the superscript “loc” in the notation).

1. Uncertainties associated to the description of the solar modulations are significant at low energy, but vanish for $E \gtrsim 20\text{--}30$ GeV, when the calculations performed with different value of the potential V become approximately equal.
2. For $E \gtrsim 30$ GeV the spectra of \bar{p} and e^+ take a simple power law form ($q_j(E) \propto E^{-\alpha_j}$) with approximately the same exponent.
3. The exponents α_{e^+} and $\alpha_{\bar{p}}$ of the positron and antiproton production rates have a value close to the spectral index of the primary proton spectrum:

$$\alpha_{\bar{p}} \simeq \alpha_{e^+} \approx \gamma_p . \quad (7)$$

This is an expected and well understood result: the energy distributions of secondaries generated by a power law spectrum of primary particles, in good approximation and sufficiently far from threshold effects, have a

power law form with the same spectral index (see also discussion below in the appendix A). Note however that equation (7) is not an exact result. This is because the primary spectrum is not a simple power law (and therefore γ_p is not exactly constant), and scaling violations in the hadronic cross sections also introduce small but non negligible (and model dependent) corrections.

4. The ratio $q_{e^+}(E)/q_{\bar{p}}(E)$ of the positrons and antiprotons injection rates is shown in Fig. 7 plotted as a function of the kinetic energy. For small energy the injection rate of positrons is much larger than for antiprotons ($q_{e^+}(E)/q_{\bar{p}}(E) \simeq 500$ at $E \simeq 1$ GeV). The ratio decreases monotonically with E and reaches an asymptotic value of order 2 for $E \gtrsim 20$ –30 GeV. This behavior can be easily understood qualitatively as a the consequence of simple kinematical effects. The production of antiprotons at low energy is suppressed because the creation of a nucleon/antinucleon pair has a relatively high energy threshold (the minimum kinetic energy of the projectile proton is $E_{0,\min} = 6 m_p$). In addition the creation of antinucleons at rest or moving backward in the laboratory frame is kinematically forbidden for any projectile energy E_0 . The importance of these kinematical effects becomes progressively less important with increasing energy, and the ratio e^+/p converges to an approximately constant value.

$$\left. \frac{q_{e^+}(E)}{q_{\bar{p}}(E)} \right|_{E \gtrsim 30 \text{ GeV}} \approx 1.8 \div 2.1 \quad (8)$$

5. Figure 7 also shows the ratio $n_{e^+}(E)/n_{\bar{p}}(E)$ of the densities of antiparticles in the local interstellar medium (estimated deconvolving the effects of solar modulations). The two ratios have energy dependences that are remarkably similar. In fact, taking into account the systematic uncertainties, the two ratios are consistent with being equal in the entire energy range:

These results can be summarized with the statement:

$$\frac{\phi_{e^+}^{\text{loc}}(E)}{\phi_{\bar{p}}^{\text{loc}}(E)} \approx \frac{q_{e^+}^{\text{loc}}(E)}{q_{\bar{p}}^{\text{loc}}(E)}. \quad (9)$$

an unexpected and intriguing result.

6. Equation (9) implies that the ratios $\tau_{e^+}(E) = n_{e^+}(E)/q_{e^+}(E)$ and $\tau_{\bar{p}} = n_{\bar{p}}(E)/q_{\bar{p}}(E)$ between the local spectra of antiparticles and the local production rates. are approximately equal. These ratios, that have the dimension of time and are of order 10^6 years, are shown in Fig. 8. Inspection of the figure suggests that the ratios have a non trivial energy dependence, most clearly in the low energy region ($E \lesssim 20$ –30 GeV). For $E \gtrsim 50$ GeV the energy dependence of the ratios appears to be weaker, and a power law description of the numerical results gives a result of order $E^{0.15 \pm 0.07}$, where the error is a rough estimate of the systematic uncertainties associated to the shape of the primary flux and of the modeling of hadronic interactions.

The quantities $\tau_j(E)$ can be related to the residence time of particles in the Galaxy, but the relation depends on the effective volume of the production and containment of the particles.

The result of equation (9) that the ratio of the production rates of positrons and antiprotons in the solar neighborhood, is (within systematic uncertainties) equal to the ratio of the fluxes of e^+ and \bar{p} is a result that naturally suggests that the local production of antiparticles is representative of the the production rate in the entire Galaxy (or in an important part of the Galaxy), and that the e^+/\bar{p} ratio at production is preserved by propagations. It is of course also possible that equation (9) is only a “coincidence”, a numerical accident of no physical significance, and that the positron and antiproton fluxes are generated by distinct source mechanisms. The implications of these two possibilities will be discussed in the following.

IV. ENERGY LOSSES

The rates of energy loss for relativistic e^\pm and p (\bar{p}) propagating in interstellar space differ by many orders of magnitude. The dominant mechanisms of energy losses are synchrotron emission and Compton scattering (where the target is formed by the radiation fields present in space: CMBR, infrared radiation and starlight). In both cases the rate energy losses depends on the mass and energy of the particles approximately as $|dE/dt| \propto E^2/m^4$, so that the effect is completely negligible for p and \bar{p} , but is potentially important for e^\pm .

The rate of energy loss of e^\mp due to synchrotron radiation is:

$$- \left. \frac{dE}{dt} \right|_{\text{syn}} = \frac{4}{3} \sigma_{\text{Th}} c \rho_B \frac{E^2}{m_e^2} \quad (10)$$

where E is the particle energy, $\rho_B = B^2/(8\pi)$ is the energy density stored in the magnetic field, and σ_{Th} is the Thomson cross section.

The energy loss for Compton scattering depends on the density and energy distribution of the photons that form the target radiation field. In a reasonably good approximation the energy loss of e^\mp for Compton scattering is given by an expression very similar to (10):

$$-\left.\frac{dE}{dt}\right|_{\text{IC}} \simeq \frac{4}{3} \sigma_{\text{Th}} c \rho_\gamma^*(E) \frac{E^2}{m_e^2} \quad (11)$$

where $\rho_\gamma^*(E)$ is the energy density in target photons that have energy below the maximum value $\varepsilon_{\text{max}} \simeq 4m_e^2/E$. This constraint insures that the $e\gamma$ scatterings are in the so called Thomson regime. Interactions with higher energy photons are in the Klein–Nishina regime, where the $e\gamma$ cross section is suppressed.

Combining the energy losses for synchrotron emission and Compton scattering, the characteristic time for energy loss for e^\mp is:

$$\begin{aligned} T_{\text{loss}}(E) &= \frac{E}{|dE/dt|} \simeq \frac{3m_e^2}{4c\sigma_{\text{Th}} \langle \rho_B + \rho_\gamma^*(E) \rangle E} \\ &\simeq 310.8 \left[\frac{\text{GeV}}{E} \right] \left[\frac{\text{eV cm}^{-3}}{\langle \rho_B + \rho_\gamma^*(E) \rangle} \right] \text{Myr} . \end{aligned} \quad (12)$$

In this equation the average $\langle \rho_B + \rho_\gamma^*(E) \rangle$ is performed along the trajectory of the particle.

The characteristic time for energy loss scales $\propto E^{-1}$, and depends on the average energy density $\langle \rho_B + \rho_\gamma^*(E) \rangle$. To estimate this energy density one can observe that the energy density of the magnetic field $\rho_B = B^2/(8\pi)$ scales as the square of the magnetic field, and for $B \simeq 3 \mu\text{G}$ (the typical strength of the magnetic field in the Galactic plane) has the value $\rho_B \simeq 0.22 \text{ eV/cm}^3$. The energy density of the radiation field can be decomposed in the sum of three main components: CMBR, dust emitted radiation and starlight. The 2.7 Kelvin Cosmic Microwave Background Radiation (CMBR) fills homogeneously all space with the energy density $\rho_{\text{CMBR}} \simeq 0.26 \text{ eV/cm}^3$. CMBR photons have the average energy $\langle \varepsilon \rangle \simeq 6.3 \times 10^{-4} \text{ eV}$, and therefore this component is effective as a target for Compton scattering up to very high energy ($E \lesssim 400 \text{ TeV}$). The dust emitted infrared radiation in the solar neighborhood has an energy density of order $\rho_\gamma \simeq 0.25 \text{ eV/cm}^3$, formed by infrared photons with an average energy of order 0.01 eV, and is effective for $E \lesssim 30 \text{ TeV}$. Finally starlight in the solar neighborhood has an energy density of order $\rho_\gamma \simeq 0.5 \text{ eV/cm}^3$, formed by photons with an average energy of 1 eV, and is effective for $E \lesssim 300 \text{ GeV}$. One can conclude that the energy loss time of an e^\mp with energy of order 1 TeV is of order 0.6 Myr if the particles remain close to the galactic plane, but can also be longer (of order of 1.2 Myr) if the particle confinement volume is much larger than the galactic disk.

V. FORMATION OF THE COSMIC RAY FLUXES

The formation of the Galactic cosmic ray fluxes can be naturally decomposed into two steps: “release” and “propagation”. In the first step, relativistic charged particles are injected or “released” in interstellar space. In the second step the particles propagate in the Galaxy from the release point to the observation point.

Assuming the validity of this decomposition, the relation between $n_j(E, \vec{x}, t)$ (the density of cosmic rays of type j and energy E present at time t at the point \vec{x}) and $q_j(E_i, \vec{x}_i, t_i)$ (the rate of release per unit volume of cosmic rays of type j and energy E_i at time t_i at the point \vec{x}_i) can be written in general as:

$$n_j(E, \vec{x}, t) = \int_{-\infty}^t dt_i \int d^3x_i \int dE_i q_p(E_i, \vec{x}_i, t_i) \times P_j(E, \vec{x}, t; E_i, \vec{x}_i, t_i) . \quad (13)$$

In this equation $P_j(E, \vec{x}, t; E_i, \vec{x}_i, t_i)$ is a propagation function that describes the probability density that a particle of type j that at the time t_i is at the point \vec{x}_i with energy E_i can be found at a later time t at the point \vec{x} with energy E . The subscript in the notation indicates that the propagation functions will in general have different forms for different particle types.

It is natural to divide the cosmic rays into two classes, according to the nature of their mechanism of interstellar release. Primary particles (such as proton, electrons, or helium nuclei) are accelerated in astrophysical sources and then ejected into interstellar space. Secondary particles (such as the rare nuclei Lithium, Beryllium and Boron) are created already relativistic as final state products in the inelastic interactions of primary cosmic rays.

Equation (13) is written in a very general form, using an absolute minimum of theoretical assumptions: it does not require that the Galactic CR are in a stationary state, it allows for CR in different points of the Galaxy to have

spectra of different shapes, it allows for energy losses or reacceleration during propagation, and leaves the propagation function to have a completely general form. Most models for the Galactic cosmic rays have to introduce several simplifying approximations.

Without loss of generality it is possible to define the current total rate of release of CR of type j as:

$$Q_j(E) = \int d^3x q_j(E, \vec{x}, t_0). \quad (14)$$

The flux of CR of type j can be written in the form:

$$\phi_j(E) \approx \frac{\beta c}{4\pi} Q_j(E) \frac{T_j(E)}{V_{\text{eff}}} \quad (15)$$

where V_{eff} is an effective Galactic volume (taken as independent from the particle type and energy), and $T_j(E)$ is an (energy dependent) quantity with the dimension of time that has to be calculated constructing a model for CR propagation in the Galaxy. The spectral shapes of CR at the Sun are determined by the combination of two effects: the properties of the sources (that determine of the release spectra), and the properties of propagation.

A. The “standard framework” for Cosmic Rays in the Galaxy

In recent years several authors have discussed the problem of the formation of the Cosmic Rays spectra in the Galaxy using a set of very similar ideas and assumptions, that can be seen as constituting a common, broadly (but not universally) accepted framework for the formation of the cosmic ray spectra. We will refer here to this set of ideas and assumptions as the “standard framework” for Cosmic Rays in the Galaxy and outline below some of the most relevant points.

- (a) Relativistic protons and electrons are released in interstellar space by the astrophysical accelerators with energy spectra that, in a broad energy range, have approximately the same shape, so that the e^-/p ratio is approximately constant.

The spectra generated by the accelerators have the same form because the particles are accelerated by a “universal” mechanism, such as Fermi Diffuse Acceleration (DSA), that operates equally on all relativistic charged particles, independently from the sign of the electric charge. The existence of such universal mechanism also insures that the spectra generated by different sources have approximately the same shape (perhaps differing only for having different maximum acceleration energies).

The difference in mass for electrons and protons results in two important effects. (i) The efficiency for injection in the acceleration mechanism (when the particles are extracted from the tail of thermal distribution of the medium) is higher for protons than for electrons. This results in a (constant) e^-/p ratio (for the release spectra) that is much smaller than unity. (ii) The maximum energy that a source can impart to electrons is expected to be smaller than the maximum energy for protons, since it corresponds to the energy for which the rates of acceleration and energy loss are equal.

- (b) The propagation of protons and nuclei is controlled by diffusion generated by the irregular Galactic magnetic field. A fundamental quantity is the residence (or escape) time $T_{\text{esc}}(E)$, that is the average time for a cosmic ray to diffuse out of the Galaxy. The escape time is a function of (the absolute value) the particle rigidity, and scales as $\propto \beta^{-1}$.

The characteristic time for protons or nuclei ($T_p(E)$ or $T_A(E)$) that enters equation (15) can be identified with the residence time.

- (c) The rigidity dependence of the CR residence time can be determined comparing the spectral shapes of primary and secondary nuclei. The comparison of the spectra of Boron and Carbon suggests the power law dependence:

$$T_{\text{esc}}(p/|Ze|) \propto \left(\frac{p}{|Ze|} \right)^{-\delta} \quad (16)$$

with $\delta \simeq 0.4-0.5$.

- (d) The difference in spectral shape between electrons and protons is a propagation effect, and is the consequence of the much larger rate of energy loss for electrons.

- (e) The e^-/p ratio start falling for E larger than few GeV. If this is the effect of different energy losses for e^- and p , one has to infer that for $E \simeq 10$ GeV, the electron residence is longer than the energy loss time (estimated in equation (12)): $T_{\text{esc}}(10 \text{ GeV}) \gtrsim 30 \text{ Myr}$.
- (f) The characteristic time $T_e(E)$ in equation (15) is a combination of the escape time $T_{\text{esc}}(E)$ and energy loss time $T_{\text{loss}}(E)$ that depends on the geometry of the space distribution of the CR accelerators and of the CR confinement volume. For the simple case where the release and confinement volume are equal one has that at large energy $T_e(E)$ coincides with $T_{\text{loss}}(E)$. More in general, for a power law energy dependence $T_e(E) \propto E^{-\delta_e}$ one has $\delta_e > \delta$.

The electron/proton ratio measure the different energy dependence of the characteristic times $T_p(E) \simeq T_{\text{esc}}(E)$ and $T_e(E)$:

$$\frac{\phi_{e^-}(E)}{\phi_p(E)} \simeq \frac{T_e(E)}{T_p(E)} \simeq \frac{T_e(E)}{T_{\text{esc}}(E)} \propto E^{-(\delta_e - \delta)}. \quad (17)$$

- (g) The spectra of CR protons and nuclei are expected to have approximately equal shape in different points of the Galaxy, while the shape of the CR electron spectrum should become softer for points distant from the Galactic plane. This is because the electron accelerators are close to the Galactic plane, and the particles lose a non negligible amount of energy during propagation.

B. Antiparticle fluxes in the “standard framework”

Using the chain of arguments outlined above it is possible to estimate the fluxes of positrons and antiprotons generated by the conventional mechanism of secondary production. The result is a predicted positron flux that is significantly softer than the observations.

It is straightforward to present the result stated above for the energy range $E \gtrsim 30$ GeV, where the CR spectra have power law form.

- The spectra of secondary positrons and antiprotons generated in hadronic interactions have approximately the same spectral index as the primary protons (and nuclei):

$$\alpha_{e^+} \simeq \alpha_{\bar{p}} \simeq \gamma_p \quad (18)$$

- The properties of propagation for e^+ and e^- are approximately equal, and similarly for p and \bar{p} . This implies that the production spectra of e^+ and \bar{p} are distorted by the propagation in distinct ways that are predicted by the observations discussed above.

The prediction for the positron/antiproton ratio is:

$$\frac{\phi_{e^+}(E)}{\phi_{\bar{p}}(E)} \simeq \frac{\phi_{e^-}(E)}{\phi_p(E)} \simeq \frac{T_e(E)}{T_{\text{esc}}(E)} \simeq E^{-(\delta_e - \delta)} \quad (19)$$

Other robust predictions are that positron spectrum should be softer than the electron spectrum, and the \bar{p} should be softer than the p spectrum, with approximately equal distortions:

$$\frac{\phi_{\bar{p}}(E)}{\phi_p(E)} \simeq \frac{\phi_{e^+}(E)}{\phi_{e^-}(E)} \simeq E^{-\delta} \quad (20)$$

The predictions presented in equation (19) and (20) are not supported by the data. The most spectacular discrepancy is for the positron flux, that is predicted to be softer than the electron one while in the data the e^+ spectrum is *harder*, in direct conflict with the prediction.

In the standard framework for CR in the Galaxy, the hard spectrum of positrons is explained introducing a new source of relativistic positrons (such as direct acceleration in Pulsars or the annihilation or decay of Dark Matter). The shape of the spectrum generated by this new positron source is harder than the spectrum of positrons generated by the conventional mechanism so that, including the softening induced by the propagation, one obtains the observed spectrum.

The new positron source cannot generate a significant spectrum of antiprotons with a spectrum of similar shape, because in the “standard framework” we are discussing here such a new source would result in an antiproton spectrum harder than the positron one, and harder than the observations.

The conclusion is that the observed positron and antiproton fluxes must be generated by distinct mechanisms, and are completely unrelated. The fact that they have the same spectral index ($\gamma_{e^+} \simeq \gamma_{\bar{p}}$ for $E > 30$ GeV) is just an accident, because these indices emerge in completely different ways. For positrons one has

$$\gamma_{e^+} \simeq \alpha_{e^+} + \delta_e \quad (21)$$

with α_{e^+} the spectral index generated by the new source, and δ_e related to the propagation effect for e^\pm , while for antiprotons

$$\gamma_{\bar{p}} \simeq \alpha_{\bar{p}} + \delta \quad (22)$$

with $\alpha_{\bar{p}}$ the spectral index that emerge from the conventional mechanism, and δ that describes propagation effects for $p(\bar{p})$.

The approximate equality of the spectral indices of positrons and antiprotons is already intriguing, but perhaps even more surprising is the fact that two unrelated mechanisms generate spectra of approximately the same absolute value, in fact that the *observed* positron/antiproton ratio (approximately 2.04 ± 0.04) is equal (within systematic uncertainties) to the ratio at *production* calculated with the conventional mechanism. The last result can in fact be extended to the broader energy range $E \in [1, 350]$ GeV, as shown in equation (9), strongly suggesting that we are not in front to a numerical coincidence and that a physical explanation is required.

VI. ALTERNATIVE FRAMEWORK

In this section we will take the point of view, that the result of equation (9) is not a numerical accident, but is an essential indication that points to a common origin for the observed fluxes of e^+ and \bar{p} , and discuss if this point of view is viable, and what are its implications.

Equation (9) shows that, taking into account statistical and systematic uncertainties, the ratio of the observed fluxes of positrons and antiprotons, is equal to the ratio for the production rate of antiparticles in the solar neighborhood, where the mechanism of production of e^+ and \bar{p} is the creation of secondaries in the hadronic interactions of primary cosmic rays. If the result is not a simple numerical coincidence, it suggests the following points:

- (i) Secondary production in hadronic interactions is indeed the source of the CR positrons and antiprotons.
- (ii) The energy dependence of the “local” (i.e. solar neighborhood) production of antiparticles is representative for the entire (or most of the) production of antiparticles, at least for our space–time point of observation.
- (iii) Propagation effects must not distort the energy dependence of the e^+/\bar{p} ratio at production. From this one can deduce two results.
 - (a) Positrons and antiprotons must propagate in approximately the same way.
 - (b) The energy of the particles must remain approximately constant during propagation. This is because the e^+ and \bar{p} production spectra have different shapes, and a significant variation of the energy of the particles during propagation would result in distinct spectral distortions for the two particle types and change the energy dependence of the ratio.

The general expressions for the formation of the spectra of cosmic rays has been given in equation (13). It is possible to express more formally the points just listed above using the same notation. Point (i) and (ii) suggest that the production rates of positrons and antiprotons have the factorized form:

$$q_{e^+(\bar{p})}(E, \vec{x}, t) \simeq q_{e^+(\bar{p})}^{\text{loc}}(E) F_q(\vec{x}, t) \quad (23)$$

so that the energy dependence of the local production is valid in the region of space and time where the production of antiparticles is important. The function $F_q(\vec{x}, t)$ that describes the space and time dependence of the antiparticles production must be equal for positrons and antiprotons. This is because, the observed fluxes of e^+ and \bar{p} are formed summing contributions produced in different points and at different times. To insure that the ratio of the observed fluxes is equal to the ratio at production, the space–time distributions of q_{e^+} and $q_{\bar{p}}$ must be equal.

In addition, as stated in point (iii), the propagation of positrons and antiproton must be (approximately) equal, and leave the energy of the antiparticles (approximately) constant. This can be obtained when the propagation functions for positrons and antiprotons in equation (13) take the form:

$$P_{e^+(\bar{p})}(E, \vec{x}_\odot, t_0; E_i, \vec{x}_i, t_i) \simeq \delta[E - E_i] P(E, \vec{x}_\odot, t_0; \vec{x}_i, t_i) \quad (24)$$

where \vec{x}_\odot is the position of the solar system in the Galaxy, t_0 the time now, and the function P is equal for positrons and antiprotons.

Inserting equations (23) and (24) in the general expression (13) for propagation one obtains, for the density of positrons and antiprotons at the present time in the vicinity of the Sun the expressions:

$$n_{e^+(\bar{p})}^{\text{loc}}(E) = q_{e^+(\bar{p})}^{\text{loc}}(E) \left[\int_{-\infty}^{t_0} dt_i \int d^3x_i F_q(E, \vec{x}_i, t_i) \times P(E, \vec{x}_\odot, t_0; \vec{x}_i, t_i) \right] \quad (25)$$

$$= q_{e^+(\bar{p})}^{\text{loc}}(E) \tau(E) \quad (26)$$

The factor in square parenthesis in the equation above has the dimension of time, and is common for positrons and antiprotons so that equation (9) is satisfied.

Is it possible to construct a model where the formation of the spectra of positrons and antiproton happens with the properties listed above? The most critical problem is the requirement that the propagation of positrons and antiproton is (at least approximately) equal. The *rates* of energy losses for the two particle types differ by many orders of magnitude, therefore the only way to insure that positrons and antiprotons have the same properties in Galactic propagation is that the residence time of the particles in the Galaxy is sufficiently short, so that the total energy loss $\Delta E \simeq |dE/dt| T_{\text{esc}}(E)$ suffered by positrons during propagation remains negligible ($\Delta E \ll E$). This requirement can also be expressed in the form:

$$T_{\text{esc}}(E) < T_{\text{loss}}(E) \lesssim 1.2 \left[\frac{1}{E_{\text{TeV}}} \right] \left[\frac{0.26 \text{ eV cm}^{-3}}{\langle \rho_B + \rho_\gamma^*(E) \rangle} \right] \text{ Myr} \quad (27)$$

where we have made use of equation (12). The numerical upper limit on the residence time is obtained setting the energy density $\langle \rho_B + \rho_\gamma^*(E) \rangle$ equal to its minimum value, that is the energy density of the CMBR that permeates uniformly space. This is possible if the confinement volume of the particles is very large, so that the contributions to the energy density of the magnetic field and of radiation generated in the Galaxy (that are concentrated near the Galactic disk) become negligible.

The upper bound on the CR residence time in equation (27) is shown graphically in Fig. 9. Is such a bound compatible with existing observations? The most direct and reliable method to estimate the residence time of cosmic rays in the Galaxy is based on the study of the ratio of the beryllium isotopes ^{10}Be and ^9Be . Both isotopes are formed as secondaries in the fragmentation of higher mass nuclei, but the beryllium-10 is unstable with an half-life of 1.51 ± 0.04 Myr [28] and acts as a cosmic-clock to measure the time elapsed from the nucleus creation [29–31]. The Cosmic Ray Isotope Spectrometer (CRIS) collaboration, using an instrument aboard the Advanced Composition Explorer (ACE) spacecraft has measured the ratio $^{10}\text{Be}/^9\text{Be}$ in the energy range $E_0 \simeq 70\text{--}145$ MeV/nucleon (with E_0 the kinetic energy per nucleon). The ratio is of order 0.11–0.12, and since the production rate of the two isotopes in the fragmentation of higher mass nuclei is approximately equal, this indicates that approximately 90% of the Beryllium-10 nuclei have decayed. The CRIS collaboration, using a “Leaky Box” theoretical framework has then estimated a residence time $T_{\text{esc}} = 15.0 \pm 1.6$ Myr for the unstable nuclei.

In order to extrapolate these results to e^\pm in the energy range of several hundred GeV, one can make the ansatz that the residence time depends on the rigidity and velocity of the particles with the (2-parameter) functional form:

$$T_{\text{res}} \approx \frac{T_0}{\beta} \left(\frac{p}{p_0 |Ze|} \right)^{-\delta_T} \quad (28)$$

(p_0 is an arbitrary scale that without loss of generality can be set to 1 GeV). The constraint that the residence time is shorter than $T_{\text{loss}}(E)$ for $E \lesssim E^*$ can then be used to set limits on the parameters δ_T and T_0 .

An intriguing possibility is to interpret the spectral break observed by the Atmospheric Cherenkov telescopes as the transition from the regime where the residence time for e^\pm is shorter than the loss time, to the regime where the opposite is true. Defining the critical energy E^* as the energy where the residence and loss time for e^\mp are equal:

$$T_{\text{loss}}(E^*) \simeq T_{\text{res}}(E^*) \quad (29)$$

one expects to observe a spectral feature in correspondence of E^* with a $\Delta\gamma$ that can be as large as unity.

Tentatively identifying the break energy observed by HESS, MAGIC and VERITAS with the critical energy E^* , one can estimate the residence time for e^\mp at the break energy, as it is equal to the loss time. The result (using the HESS estimate for the energy of the break energy):

$$T_{\text{res}}(900 \text{ GeV}) \simeq T_{\text{loss}}(900 \text{ GeV}) \simeq 1.0 \pm 0.4 \text{ Myr} \quad (30)$$

where the error was estimated taking into account a 20% uncertainty in the energy scale, and a range of possible values for $\langle\rho_B + \rho_\gamma^*\rangle$ in equation (12).

Combining the two measurements of the CR residence time obtained at different rigidities, performed by CRIS using the beryllium ratio [31], and by the Air Cherenkov telescopes, and comparing to equation (28), one can estimate the two parameters T_0 and δ_T obtaining the results: $T_0 \simeq 14.0 \pm 0.4$ Myr and $\delta \simeq 0.40 \pm 0.04$.

The rigidity dependence of the residence time obtained in this estimate is actually consistent with the indications obtained from the ratio $q_j^{\text{loc}}(E)/n_j^{\text{loc}}(E)$ discussed in section III and shown in Fig. 8.

The tentative conclusion is that an interpretation of the positron and antiproton flux as entirely of secondary origin is in fact viable, and also offers a simple and attractive interpretation for the softening of the e^\pm spectrum observed by the Cherenkov telescopes.

Estimates of the residence time of cosmic rays in the Galaxy have been obtained from the study of ratio Boron/Carbon [21, 32–35]. Recently the AMS02 [36] has presented preliminary results also on the Lithium spectrum that show a striking hardening of the spectrum at a rigidity of order 300 GV, with a variation of the spectral index $\Delta\gamma \simeq 0.5$ – 0.6 . A common interpretation of the Boron and Lithium results is at the moment problematic, and a discussion of the secondary nuclei results will be postponed to wait for the publication of the Lithium results.

An additional difficulty for the interpretation of the results on secondary nuclei is that this studies do not measure directly the residence time of the nuclei, but rather the column density crossed by during propagation. The results therefore have to take into account the possibility that a significant fraction of the column density is traversed not in interstellar space but inside or close to the sources that accelerate the primary nuclei [37–39].

VII. OUTLOOK

In this work we have shown and discussed the existence of some surprising properties of CR positrons and antiprotons. The ratio e^+/\bar{p} of the antiparticles fluxes falls monotonically with energy from a value of order 100 for kinetic energy $E \simeq 1$ GeV, to a value of approximately two for $E \simeq 25$ GeV, and then remains approximately constant at the value 2.04 ± 0.04 in the energy interval 30–350 GeV (up to the highest energy of the observations). This is exactly the same behaviour of the ratio e^+/\bar{p} for the production rates of antiparticles calculated using the conventional mechanism where e^+ and \bar{p} are created as secondary products in the inelastic interactions of primary cosmic rays.

Many models for the CR antiparticles claim that the positrons are generated by a new source, that is distinct and unrelated to the (conventional) mechanism that generates antiprotons. If this interpretation is correct, then the results described above have to be considered as numerical accidents of no physical significance.

The alternative is to construct a model where positrons and antiprotons are generated by the conventional mechanism, and where the e^+/\bar{p} ratio at production is preserved during propagation. In this paper we have shown that this second possibility is viable, and implies that the CR residence time for p , \bar{p} and e^\mp is of order 0.6–1.2 Myr at energy $E \simeq 1$ TeV. This interpretation also suggests that the break in the $(e^+ + e^-)$ spectrum observed by the Atmospheric Cherenkov telescopes corresponds to the critical energy where the residence time and the loss time for CR e^\mp are equal.

Several authors (see for example [40]) have discussed models where the hard positron spectrum has its origin in the presence of a near source of particles, in order to avoid the effects of energy losses. These class of solution do not really address in a satisfactory way the puzzle that we are discussing in this work, where the key observations is the close relation between the positron and the antiproton fluxes. To preserve the ratio e^+/\bar{p} at production for the flux, the space distribution of the sources of the two particles must be approximately equal. A local source of secondary positrons and antiprotons can be a viable solution but only if it accounts for most of the fluxes for both particles. If antiprotons can reach the Sun from large distances and positrons (because of large energy losses) cannot, this would change the ratio at production, unless the contribution from all distant sources is negligible for both antiparticle type.

The CR electron spectrum is much softer than the proton spectrum in the energy region considered above. If the propagation of e^\mp and protons is approximately equal for $E \lesssim 1$ TeV, the difference in spectral shape for electrons and protons cannot be attributed to a propagation effect, and it becomes necessary to assume that the CR accelerators release electrons to interstellar space with an energy spectrum much softer than for protons. This would be a result of great importance for our understanding of the CR sources.

The solution of this puzzle, that is the identification of the mechanisms that generate positrons and antiprotons and the determination of the properties of Galactic propagation for relativistic particles, is a task of great importance for high energy astrophysics because it has implications that are broad and touch some of the cornerstones of the field.

Several lines of study have the potential to contribute to solution of the problem.

Perhaps the simplest idea is to extend the measurements of the positron flux to a broader energy range. In the model we have discussed above the spectral feature observed by the Cherenkov telescopes should be present with

the same shape for both electrons and positrons, while in the standard framework the high energy behavior of the positron flux is determined by the properties of the new source and can have different spectral shapes.

In the standard framework, the energy spectrum of electrons in points that are distant from the Galactic plane is softer than the spectrum measured close to the plane. This is because the sources of the CR electrons are in the Galactic disk, and the particles need time (and lose energy) to propagate to distant points. In models where the CR propagation is rapid, the space dependence of the CR electron spectral shape is less important.

Information about the density and spectral shape of CR e^\mp in the Galaxy can be obtained from a study of the angular and energy distribution of the diffuse gamma-ray flux [41], and also from the mapping of the radio emission. The reconstruction of the energy and space distributions of CR electrons is not an easy task, and requires a sufficiently accurate understanding of the distributions of matter, radiation and magnetic field in the Galaxy, but has great potential and should be considered as very important.

A third interesting line of study is associated to multi-wavelength studies of the sources where cosmic rays are accelerated. A careful study of these objects can perhaps give valuable information on the size and spectral shapes of the populations of CR particles of different type that are released in interstellar space.

Appendix A: Analytic estimate of the e^+/\bar{p} ratio at production

If a power law spectrum of protons ($N_p(E) \simeq K_p E^{-\gamma_p}$) interacts with a diluted gas target, the spectra of high energy positrons and antiprotons generated as secondary in the interactions have the following properties:

- (a) The e^+ and \bar{p} spectra [$\dot{N}_{e^+}(E)$ and $\dot{N}_{\bar{p}}(E)$] in good approximation, have also power law form, with exponents that are approximately equal to each other and also equal to the spectral index of the parent proton spectrum.
- (b) The constant e^+/\bar{p} ratio has a value that depends on the spectral index of the proton flux. For $\gamma_p \simeq 2.8 \pm 0.1$ (the exponent of the CR protons observed at the Earth), the ratio takes the value $e^+/\bar{p} \simeq 1.8 \pm 0.5$ where the uncertainty takes also into account an estimate of the uncertainties in the modeling of hadronic interactions.

This appendix outlines a simple analytic derivation of these two results.

Point (a) is a well known ‘‘textbook’’ result, that is in fact valid for all secondary products of hadronic inelastic collisions. It can be derived as a consequence of the approximate validity of Feynman scaling in the forward kinematical region for the inclusive spectra of secondaries in high energy hadronic interactions.

The rate of production of secondaries of type j in pp interactions can be calculated performing the integral:

$$\dot{N}_{pp \rightarrow j}(E) = n_p^{\text{target}} \int_E^\infty dE_0 N_p(E_0) \beta c \sigma_{pp}(E_0) \frac{dN_{pp \rightarrow j}}{dE}(E, E_0) . \quad (\text{A1})$$

where $N_p(E_0)$ is the spectrum of interacting protons, n_p^{target} is the density of target protons, $\sigma_{pp}(E_0)$ is the inelastic pp cross section, and $dN_{pp \rightarrow j}/dE$ is the inclusive spectrum of secondaries of type j produced in one inelastic collision. Without loss of generality one can write the inclusive spectra in the form:

$$\frac{dN_{pp \rightarrow j}}{dE}(E, E_0) = \frac{1}{E_0} F_{pp \rightarrow j}\left(\frac{E}{E_0}, E_0\right) . \quad (\text{A2})$$

The approximate validity of Feynman scaling implies that when the ratio $x = E/E_0$ not too small (i.e. in the forward region), the function $F_{pp \rightarrow j}$ depends only on x (and is independent from E_0). For a primary proton spectrum that is a power law: $N_p(E_0) = K_p E_0^{-\gamma_p}$ setting $\beta \simeq 1$, and neglecting the logarithmic energy dependence of $\sigma_{pp}(E_0)$ one can rewrite equation (A1) as:

$$\dot{N}_{pp \rightarrow j}(E) = K_p n_p^{\text{target}} c \sigma_{pp} Z_{pp \rightarrow j}(\gamma) E^{-\gamma_p} = K_j E^{-\gamma_p} \quad (\text{A3})$$

where the ‘‘Z-factor’’ $Z_{pp \rightarrow j}(\gamma)$ is:

$$Z_{pp \rightarrow j}(\gamma, E) = \int_0^1 dx x^{\gamma-1} F_{pp \rightarrow j}(x) \quad (\text{A4})$$

The final result is that the production rate of particle j is described by a power law with spectral index $\gamma_j = \gamma_p$, as stated in point (a).

It should be noted that this result is not exact, because it has been obtained making use of two approximations: the pp inelastic cross section σ_{pp} is constant, and the distribution $F_{pp \rightarrow j}$ is exactly scaling. A numerical calculation performed without these simplifying approximations results in secondary spectra with small deviations from an exact power law.

A realistic calculation must also include the fact that the parent proton spectrum is not an exact power law. In fact the CR proton and helium spectra have a spectral hardening (with a variation of the spectral index of order $\Delta\gamma_p \sim 0.15$) at a rigidity of order 200–300 GV [6, 8, 9]. Secondaries of energy E are injected by a broad distribution of primary energies that extends from E_0 just above E to $E_0 \approx 100 E$. The spectral structure of the primary particles generates also a similar, but more gradual hardening for the secondary spectra.

Using the same approximations discussed above, the ratio between the positron and anti-proton production rates is given by the ratio of the corresponding Z-factors.

$$\frac{\dot{N}_{pp \rightarrow e^+}}{\dot{N}_{pp \rightarrow \bar{p}}} \simeq \frac{Z_{pp \rightarrow e^+}(\gamma_p)}{Z_{pp \rightarrow \bar{p}}(\gamma_p)} \quad (\text{A5})$$

The production of positrons in hadronic interactions is dominated by the production and chain decay of mesons, and the function $F_{pp \rightarrow e^+}(x)$ can be written as a sum of terms that describe the production and decay of different parent mesons:

$$F_{pp \rightarrow e^+}(x) = \sum_{h \in \{\pi^+, K^+, K_L\}} F_{pp \rightarrow h \rightarrow e^+}(x) = \sum_{h \in \{\pi^+, K^+, K_L\}} F_{pp \rightarrow h}(x) \otimes F_{h \rightarrow e^+}(x) . \quad (\text{A6})$$

In this equation the symbol \otimes indicate convolution and the functions $F_{i \rightarrow e^+}(x)$ are the inclusive spectra of positrons in the decay of parent meson of type i . For ultrarelativistic particles these functions depend only on the ratio E/E_i between the positron and the parent meson energies.

The Z -factor for positron production in pp interactions can then be written as a sum of products:

$$Z_{pp \rightarrow e^+}(\gamma) = \sum_{i \in \{\pi^+, K^+, K_L\}} Z_{pp \rightarrow i}(\gamma) Z_{i \rightarrow e^+}(\gamma) \quad (\text{A7})$$

where the decay Z -factors are:

$$Z_{i \rightarrow e^+}(\gamma) = \int_0^1 dx x^{\gamma-1} F_{i \rightarrow e^+}(x) . \quad (\text{A8})$$

The decay spectrum of positrons in the chain decay of π^+ can be calculated analytically. The calculation involves using the non-trivial matrix element for 3-body muon decay, and requires to take into account the fact that the muon created in the first decay is in a well defined polarization state. The corresponding $Z_{\pi^+ \rightarrow \mu^+ \rightarrow e^+}$ factor has also an exact analytic expression [17]:

$$Z_{\pi^+ \rightarrow e^+}(\gamma) = \frac{4 [(\gamma(r_\pi - 1) + 2r_\pi - 3)r_\pi^\gamma - 2r_\pi + 3]}{\gamma^2(\gamma + 2)(\gamma + 3)(r_\pi - 1)^2} \quad (\text{A9})$$

with $r_\pi = (m_\mu/m_\pi)^2$. Similarly it is possible to calculate the decay spectra and the corresponding Z factors for the decay of kaons.

For an exponent $\gamma = 2.8$ (a value close to the observed spectrum of hadronic cosmic rays) the decay Z factors for the different mesons are: $Z_{\pi^+ \rightarrow e^+} \simeq 0.1219$, $Z_{K^+ \rightarrow e^+} \simeq 0.0563$, $Z_{K_L \rightarrow e^+} \simeq 0.0354$ (also K^- can produce positrons via the chain decay $K^- \rightarrow \pi^+ \rightarrow e^+$, but the channel is strongly suppressed $Z_{K^- \rightarrow e^+} \simeq 0.0010$). The positrons created in pion decay have a harder spectrum, and therefore a larger Z -factor. The production of kaons in hadronic interaction is suppressed by approximately a factor of 10 with respect to the production of pions. Combining this fact with the softer spectra of the positrons created in kaon decay (that results in additional suppression by a factor 2 or 3) one finds that approximately 90% of the positron injection is due to the production of positive pions, with the rest due to the kaon contribution.

The inclusive differential cross section for the production of antiprotons and pions can be approximately fitted [25, 42] with the simple functional form:

$$F_{pp \rightarrow h}(x) \simeq A_h \frac{(1-x)^{\eta_h}}{x} \simeq \langle x_h \rangle (\eta_h + 1) \frac{(1-x)^{\eta_h}}{x} \quad (\text{A10})$$

that depends on the two parameters $\{A_h, \eta_h\}$, or equivalently $\{\langle x_h \rangle, \eta_h\}$. The quantity $\langle x_h \rangle = \langle E_h \rangle / E_0$ is the average fraction of the projectile energy E_0 carried by hadrons of type h in the final state. The corresponding Z -factors are:

$$Z_{pp \rightarrow h}(\gamma) = \langle x_h \rangle (n_h + 1) \frac{\Gamma(\gamma - 1) \Gamma(n_h + 1)}{\Gamma(\gamma + n_h)} . \quad (\text{A11})$$

One now all the elements to obtain a simple estimate of the e^+/\bar{p} ratio:

$$\frac{\dot{N}_{pp \rightarrow e^+}}{\dot{N}_{pp \rightarrow \bar{p}}} \simeq \frac{Z_{pp \rightarrow e^+}(\gamma_p)}{Z_{pp \rightarrow \bar{p}}(\gamma_p)} \simeq \frac{Z_{pp \rightarrow \pi^+}(\gamma_p) \times Z_{\pi^+ \rightarrow e^+}(\gamma_p)}{Z_{pp \rightarrow \bar{p}}(\gamma_p)} \times 1.1 \quad (\text{A12})$$

In this expression γ_p is the spectral index of the proton flux, and the last factor 1.1 takes into account a 10% kaon contribution to the positron flux. Using the expression of equation (A11) for $Z_{pp \rightarrow h}$ one obtains:

$$\frac{\dot{N}_{pp \rightarrow e^+}}{\dot{N}_{pp \rightarrow \bar{p}}} \simeq \frac{\langle x_{\pi^+} \rangle}{\langle x_{\bar{p}} \rangle} \left[\frac{\Gamma(\gamma + \eta_{\bar{p}}) \Gamma(\eta_{\pi^+} + 2)}{\Gamma(\gamma + \eta_{\pi^+}) \Gamma(\eta_{\bar{p}} + 2)} \right] Z_{\pi^+ \rightarrow e^+}(\gamma) \times 1.1 \quad (\text{A13})$$

In this expression one can identify four factors. The first one $\langle x_{\pi^+} \rangle / \langle x_{\bar{p}} \rangle$ is the ratio of the energy fractions transferred to \bar{p} or π^+ (the dominant source of positrons) by the primary particle. A rough estimate for this factor is of order 9.1 ± 1.5 , where the central value has been estimated for $\langle x_{\pi^+} \rangle \simeq 0.165$. and $\langle x_{\bar{p}} \rangle \simeq 0.020$.

The second factor (in square parenthesis and written as a combination of Γ functions) takes into account the shapes of the primary proton spectrum and of the inclusive production cross sections for \bar{p} and π^+ . It depends on the spectral index γ_p of the proton spectrum, and on the parameters $\eta_{\bar{p}}$ and η_{π^+} that determine the shapes of the energy spectra

of antiprotons and positrons in the final state. This factor is larger than unity, because on average the secondary antiprotons are softer than charged pions ($\eta_{\bar{p}} > \eta_{\pi^+}$). For $\gamma_p \simeq 2.8$, $\eta_{\pi^+} \simeq 3.5$ and $\eta_{\bar{p}} \simeq 7$, the factor is approximately 1.5. Distortions of the secondary particle spectra (changes in the exponents $\Delta p \simeq \pm 1.0$) and changes in the spectral index of the primary flux $\Delta\gamma_p \simeq \pm 0.1$ can change the value of this factor by ± 0.4 .

The third factor [$Z_{\pi^+ \rightarrow e^+}^{-1}(\gamma_p)$] is the kinematical suppression factor for e^+ production due to the fact that positrons carry only a fraction of the π^+ energy and is given in equation (A9). Assuming $\gamma_p \simeq 2.8$ with an uncertainty of order ± 0.1 one obtains the estimate 0.12 ± 0.01 .

The last factor (1.1) in equation (A13) takes into account a kaon contribution to the positron flux of approximately 10%.

Putting together the results outlined above one arrives to the estimate:

$$\frac{\dot{N}_{pp \rightarrow \bar{p}}}{\dot{N}_{pp \rightarrow e^+}} \simeq (9.1 \pm 1.5) \times (1.5 \pm 0.4) \times (0.12 \pm 0.01) \times (1.10 \pm 0.02) \simeq 1.80 \pm 0.5 \quad (\text{A14})$$

This completes the derivation of the prediction (b).

Naively one could expect that the ratio positron/antiproton should be significantly larger than two, because the average number of positrons created in hadronic interactions is much larger than the number of antiprotons. However, we are not calculating the ratio of the total numbers of e^+ and \bar{p} , but the ratio of the numbers of particles with the same energy E . The production rate of positrons is suppressed with respect to antiprotons because the e^+ are produced in the chain decay of parent mesons and have a much softer spectrum. The ratio e^+/\bar{p} ratio of order two emerges as the combination of a much larger positron multiplicity per interaction, and a softer positron spectrum.

-
- [1] O. Adriani *et al.* [PAMELA Collaboration], *Nature* **458**, 607 (2009) [arXiv:0810.4995 [astro-ph]].
- [2] O. Adriani *et al.* [PAMELA Collaboration], *Phys. Rev. Lett.* **111**, 081102 (2013) [arXiv:1308.0133 [astro-ph.HE]].
- [3] O. Adriani *et al.* [PAMELA Collaboration], *Phys. Rev. Lett.* **105**, 121101 (2010) [arXiv:1007.0821 [astro-ph.HE]].
- [4] M. Ackermann *et al.* [Fermi-LAT Collaboration], *Phys. Rev. Lett.* **108**, 011103 (2012) [arXiv:1109.0521 [astro-ph.HE]].
- [5] M. Aguilar *et al.* [AMS Collaboration], *Phys. Rev. Lett.* **113**, 121102 (2014).
- [6] A. Kounine, Talk at “AMS Days at CERN” available at <http://indico.cern.ch/event/381134/> (2015)
- [7] O. Adriani *et al.* [PAMELA Collaboration], *Phys. Rev. Lett.* **106**, 201101 (2011) [arXiv:1103.2880 [astro-ph.HE]].
- [8] O. Adriani *et al.* [PAMELA Collaboration], *Science* **332**, 69 (2011) [arXiv:1103.4055 [astro-ph.HE]].
- [9] M. Aguilar *et al.* [AMS Collaboration], *Phys. Rev. Lett.* **114**, 171103 (2015).
- [10] Y. S. Yoon *et al.*, *Astrophys. J.* **728**, 122 (2011) [arXiv:1102.2575 [astro-ph.HE]].
- [11] A. A. Abdo *et al.* [Fermi-LAT Collaboration], *Phys. Rev. Lett.* **102**, 181101 (2009) [arXiv:0905.0025 [astro-ph.HE]].
- [12] F. Aharonian *et al.* [HESS Collaboration], *Phys. Rev. Lett.* **101**, 261104 (2008) [arXiv:0811.3894 [astro-ph]].
- [13] F. Aharonian *et al.* [HESS Collaboration], *Astron. Astrophys.* **508**, 561 (2009) [arXiv:0905.0105 [astro-ph.HE]].
- [14] H. S. Ahn *et al.*, *Astrophys. J.* **714**, L89-L93 (2010). [arXiv:1004.1123 [astro-ph.HE]].
- [15] D. Borla Tridon *et al.* [MAGIC Collaboration], arXiv:1110.4008 [astro-ph.HE].
- [16] D. Staszak [VERITAS Collaboration], arXiv:1508.06597 [astro-ph.HE].
- [17] P. Lipari, M. Lusignoli and D. Meloni, *Phys. Rev. D* **75**, 123005 (2007) [arXiv:0704.0718 [astro-ph]].
- [18] M. Aguilar *et al.* [AMS Collaboration], *Phys. Rev. Lett.* **113**, 221102 (2014). doi:10.1103/PhysRevLett.113.221102
- [19] M. Aguilar *et al.* [AMS Collaboration], *Phys. Rev. Lett.* **115**, no. 21, 211101 (2015). doi:10.1103/PhysRevLett.115.211101
- [20] T. K. Gaisser, T. Stanev and S. Tilav,
“Cosmic Ray Energy Spectrum from Measurements of Air Showers,” arXiv:1303.3565 [astro-ph.HE].
- [21] J. J. Engelman, P. Ferrando, A. Soutoul, P. Goret and E. Juliusson, *Astron. Astrophys.* **233**, 96 (1990).
- [22] L. J. Gleeson and W. I. Axford, *Astrophys. J.* **154**, 1011 (1968).
- [23] P. Lipari, arXiv:1408.0431 [astro-ph.HE].
- [24] L. C. Tan and L. K. Ng, *Phys. Rev. D* **26**, 1179 (1982).
- [25] G. D. Badhwar, S. A. Stephens and R. L. Golden, *Phys. Rev. D* **15**, 820 (1977).
- [26] T. Anticic *et al.* [NA49 Collaboration], *Eur. Phys. J. C* **68**, 1 (2010) [arXiv:1004.1889 [hep-ex]].
- [27] T. Sjostrand, S. Mrenna and P. Z. Skands, *JHEP* **0605**, 026 (2006) [hep-ph/0603175].
- [28] D. R. Tilley, J. H. Kelley, J. L. Godwin, D. J. Millener, J. E. Purcell, C. G. Sheu and H. R. Weller, *Nucl. Phys. A* **745**, 155 (2004).
- [29] M. Garcia-Munoz, G.M. Mason & J.A. Simpson *Astrophys. J.* **217**, 859 (1977).
- [30] S.P. Ahlen *et al.* *Astrophys. J.* **534**, 757 (2000).
- [31] N.E. Yanasak *et al.* *Astrophys. J.* **563**, 768 (2001).
- [32] G. A. de Nolfo *et al.*, *Adv. Space Res.* **38**, 1558 (2006) [astro-ph/0611301].
- [33] H. S. Ahn *et al.*, *Astropart. Phys.* **30**, 133 (2008) [arXiv:0808.1718 [astro-ph]].
- [34] A. Obermeier, P. Boyle, J. Horandel and D. Muller, *Astrophys. J.* **752**, 69 (2012) [arXiv:1204.6188 [astro-ph.HE]].
- [35] O. Adriani *et al.*, *Astrophys. J.* **791**, no. 2, 93 (2014) [arXiv:1407.1657 [astro-ph.HE]].
- [36] L. Derome, Talk at “AMS Days at CERN” available at <http://indico.cern.ch/event/381134/> (2015)
- [37] R. Cowsik and B. Burch, *Phys. Rev. D* **82**, 023009 (2010).
- [38] R. Cowsik, B. Burch and T. Madziwa-Nussinov, *Astrophys. J.* **786**, 124 (2014) [arXiv:1305.1242 [astro-ph.HE]].
- [39] R. Cowsik and T. Madziwa-Nussinov, arXiv:1505.00305 [astro-ph.HE].
- [40] H. Yuksel, M. D. Kistler and T. Stanev, *Phys. Rev. Lett.* **103**, 051101 (2009) doi:10.1103/PhysRevLett.103.051101 [arXiv:0810.2784 [astro-ph]].
- [41] [Fermi-LAT Collaboration], “Fermi-LAT Observations of the Diffuse Gamma-Ray Emission: Implications for Cosmic Rays and the Interstellar Medium,” *Astrophys. J.* **750**, 3 (2012) [arXiv:1202.4039 [astro-ph.HE]].
- [42] A. E. Brenner *et al.*, *Phys. Rev. D* **26**, 1497 (1982).

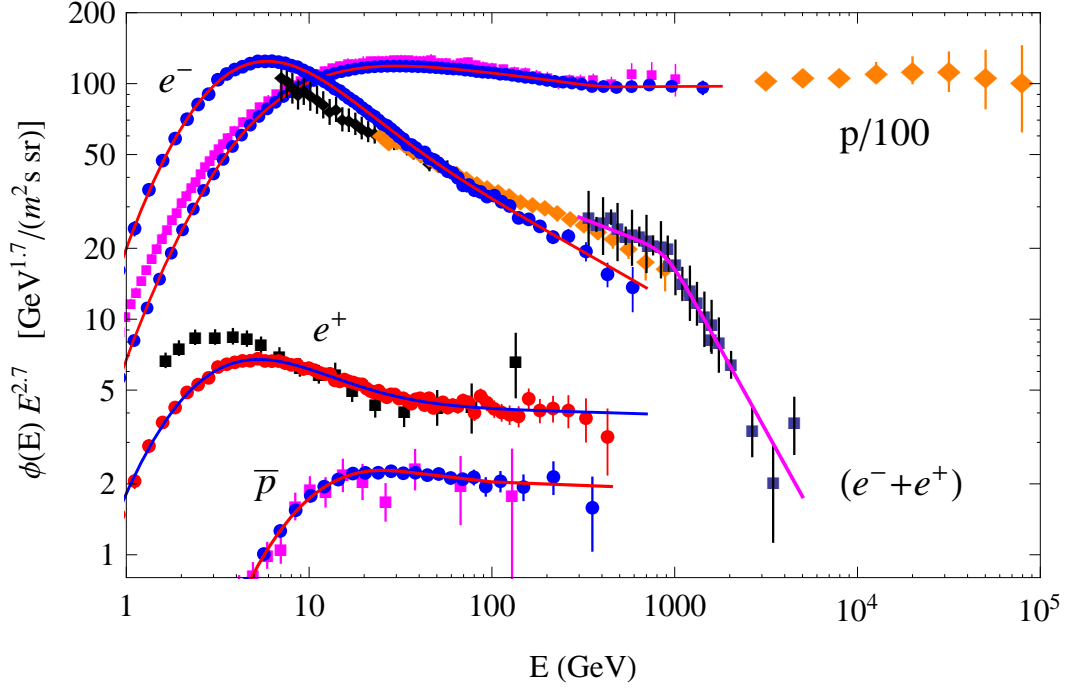


FIG. 1: Fluxes of p , e^- , e^+ and \bar{p} . The fluxes are shown in the form $\phi_j(E) E^{2.7}$ versus E (with E the kinetic energy) to enhance the features of the energy dependence. The proton data (rescaled by a factor 10^{-2}) is from PAMELA (squares) [8], AMS02 (circles) [9] and CREAM (diamonds) [10]. The electron data is from AMS02 [5]. The positron data is from PAMELA (squares) [2] and AMS02 (circles) [5]. The $(e^- + e^+)$ data is from FERMI (diamonds) [11] and HESS (squares) [12, 13]. The antiproton data is from PAMELA (squares) [3] and AM02 (circles)[6]. The lines are fit to the AMS02 data, and to the HESS $(e^- + e^+)$ data

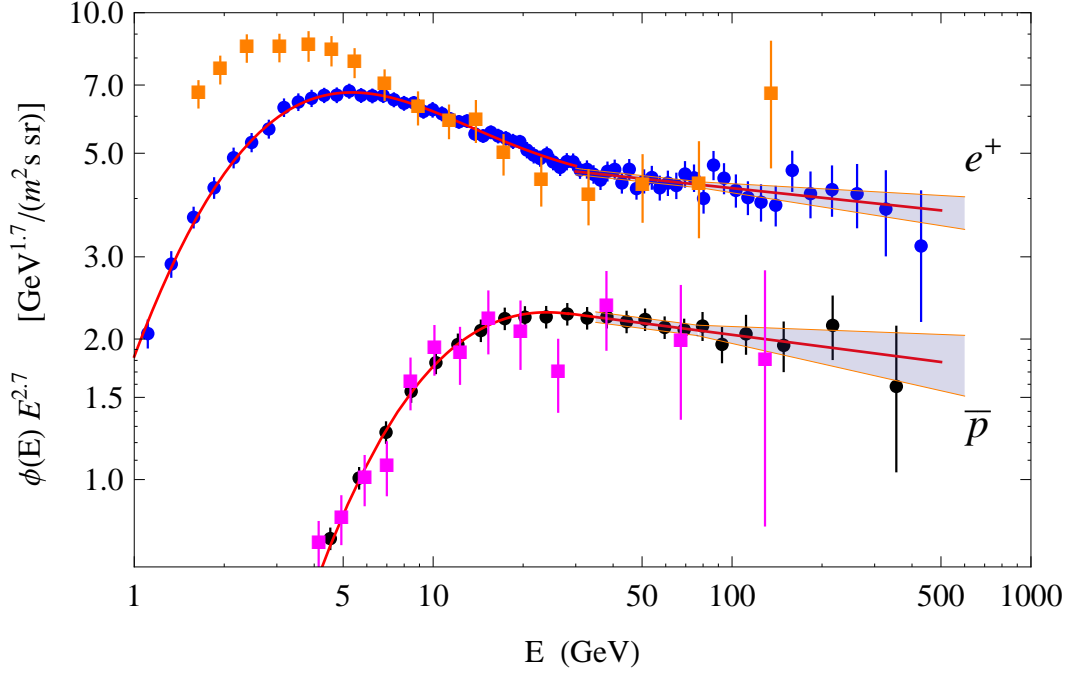


FIG. 2: Fluxes of e^+ and \bar{p} shown in the form $\phi_j(E) E^{2.7}$ versus E . The circles are measurements by AMS02 [5], [6]. The squares are measurements by PAMELA [2] and [3]. The lines are smooth fits to the AMS02 data. The band indicate the range of power law fits to the AMS02 data in the range $E > 30$ GeV (see text).

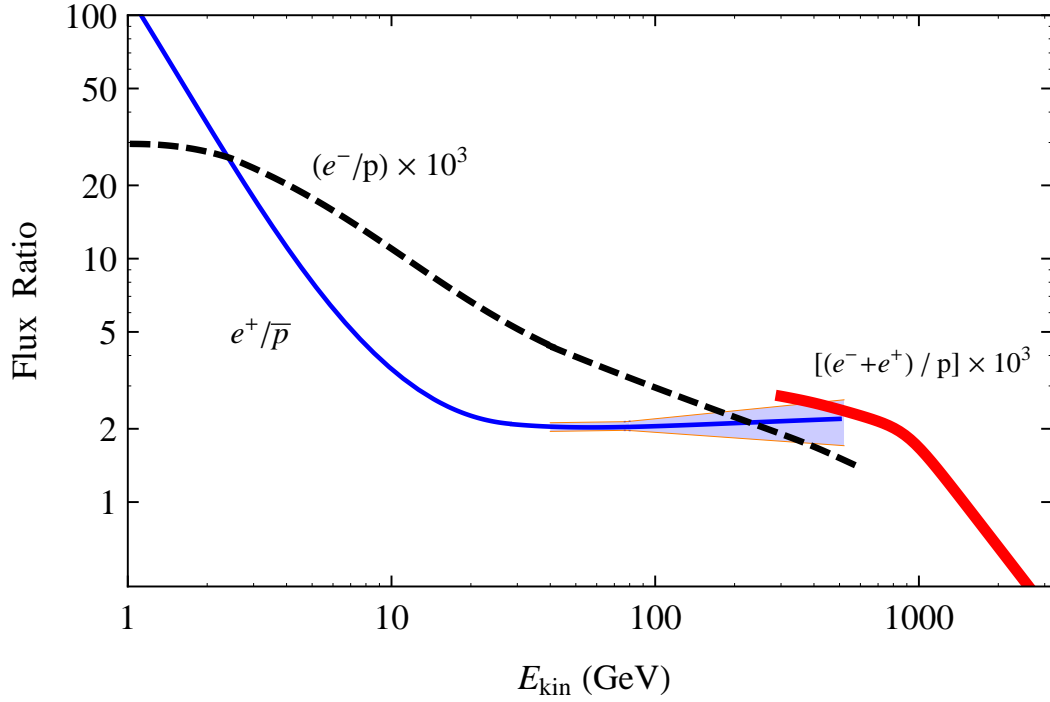


FIG. 3: Ratios e^+/\bar{p} , e^-/p , and $(e^- + e^+)/p$ between the fluxes of different particle types. All lines are ratios of the fits to the experimental data shown in Fig. 1 and Fig. 2. For the e^+/\bar{p} ratio the fit given in equation (4) is also shown.

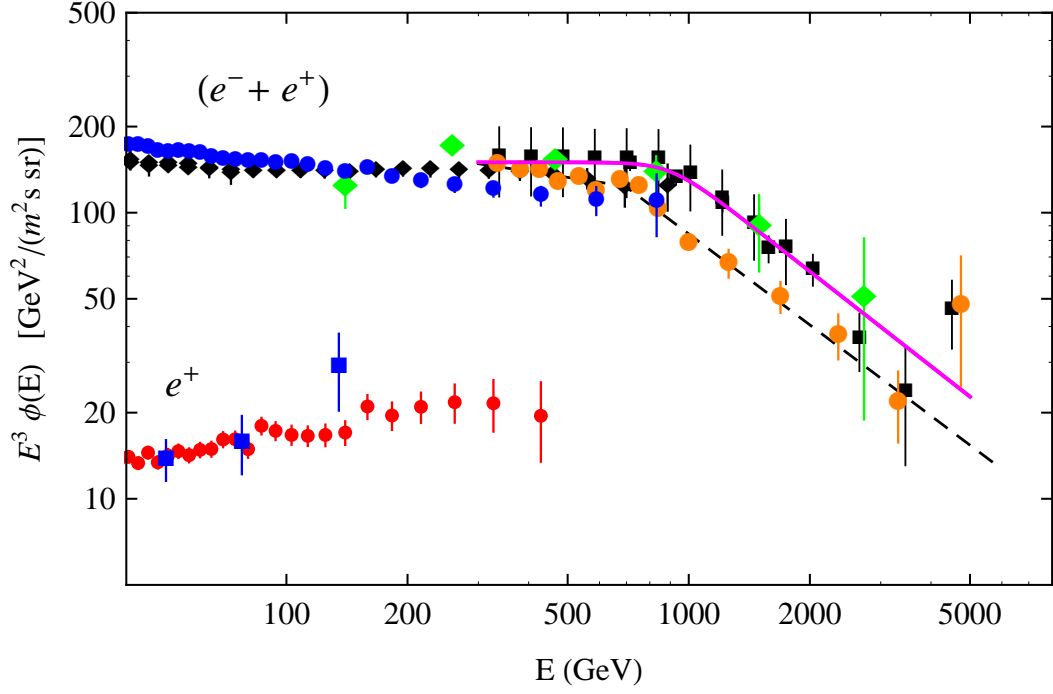


FIG. 4: Flux measurements of the sum ($e^+ + e^-$) obtained by AMS02 (small circles) [18], FERMI (small diamonds), HESS (squares), MAGIC (diamonds) and VERITAS (big circles). The solid (dashed) line is the best fit to the data obtained by HESS [13] (VERITAS [16]).

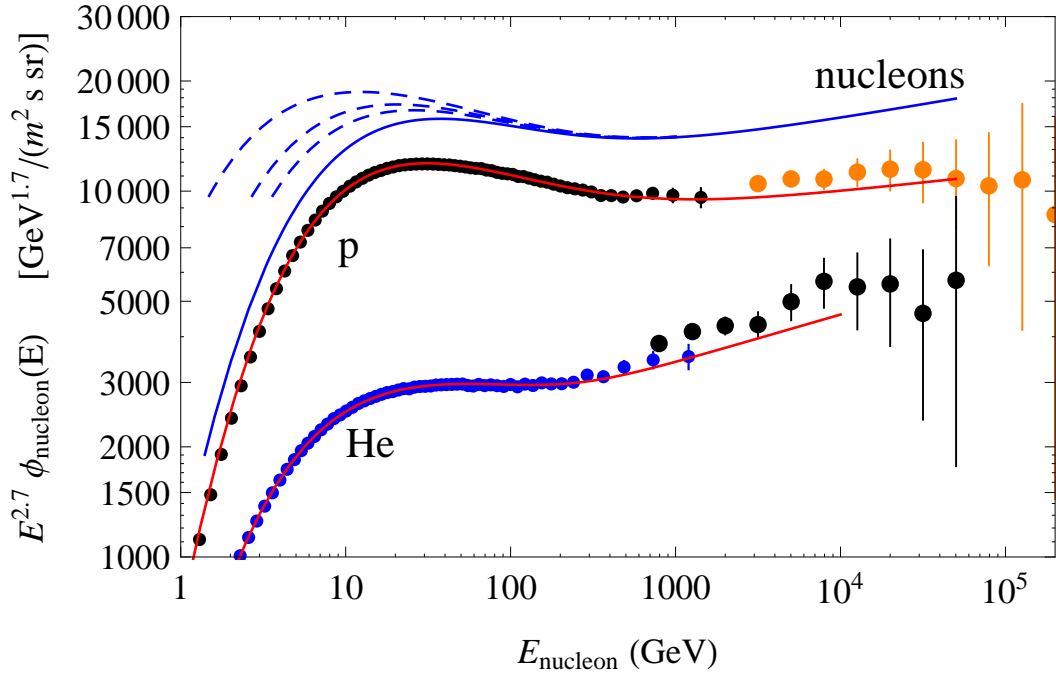


FIG. 5: Interstellar spectra for protons and helium used in this work. The data points are measurements performed by AMS02 (small circles) [9, 19] and CREAM (big circles) [10]. The lines show the all nucleon flux at the Earth) solid line and in interstellar space. To correct for solar modulation effects the potential has been estimated as $V = 0.4, 0.6$ and 0.9 GV.

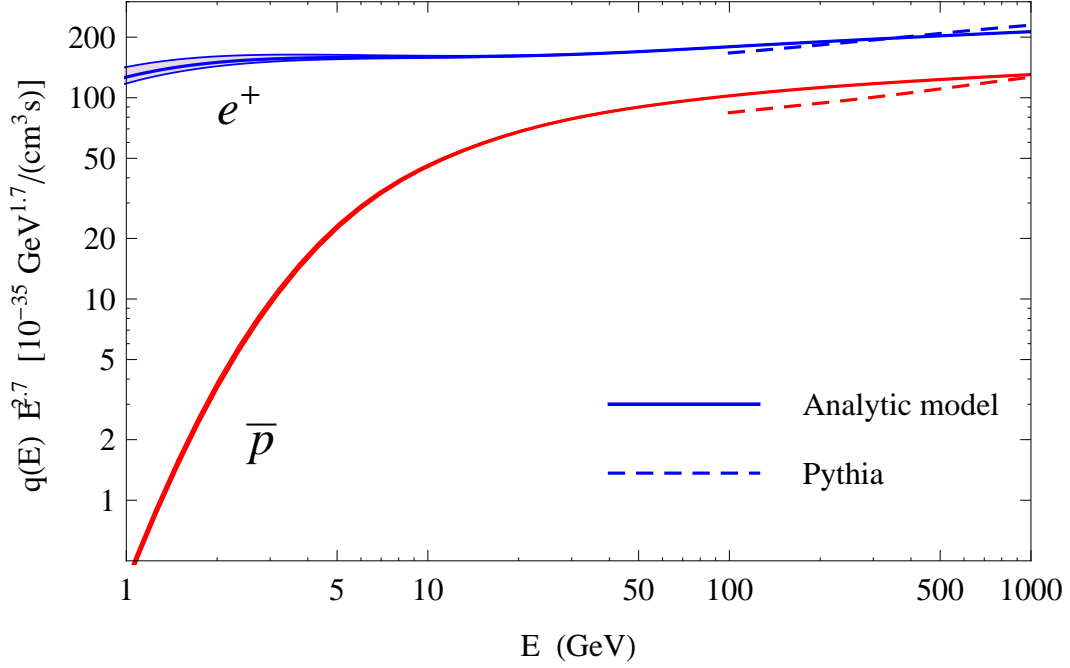


FIG. 6: Production rates of \bar{p} and e^+ calculated with the conventional mechanism in the solar neighborhood. The production rates have been calculated using two methods: an analytic description of the differential hadronic cross sections [24–26], and (for $E > 100$ GeV) the Pythia Monte Carlo code [27].

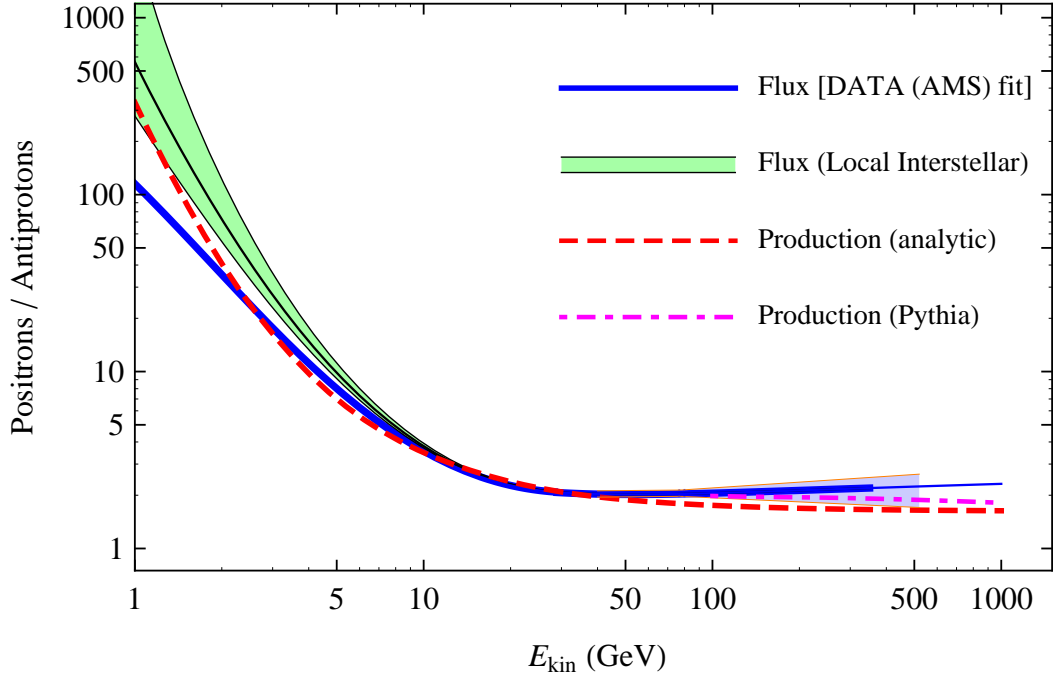


FIG. 7: Ratio e^+/\bar{p} as a function of the kinetic energy. The thick line shows the ratio $\phi_{\bar{p}}(E)/\phi_{e^+}(E)$ of the fluxes observed at the Earth (the line is also shown in Fig. 3). The ratio of the fluxes in interstellar space is shown as a shaded are, and was calculated correcting for the solar modulation effects using three different values of the solar modulation parameter ($V = 0.4, 0.6$ and 0.9 GV). The dashed line is the calculated ratio of the production rates of positrons and antiprotons in the solar neighborhood. For $E > 100$ GeV also the results of calculation performed using the Pythia Monte Carlo code is shown.

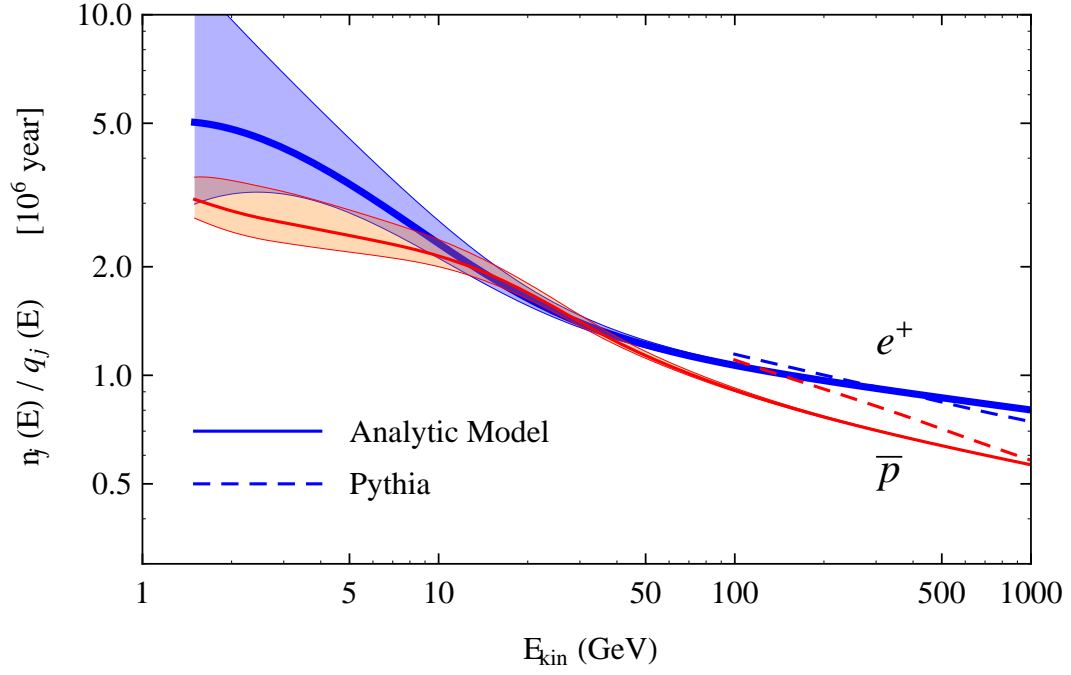


FIG. 8: Ratio $n_j(E)/q_j(E)$ (with $j = \bar{p}, e^+$) between the measured cosmic ray density and the production rate in the solar neighborhood calculated in the conventional model of secondary production.

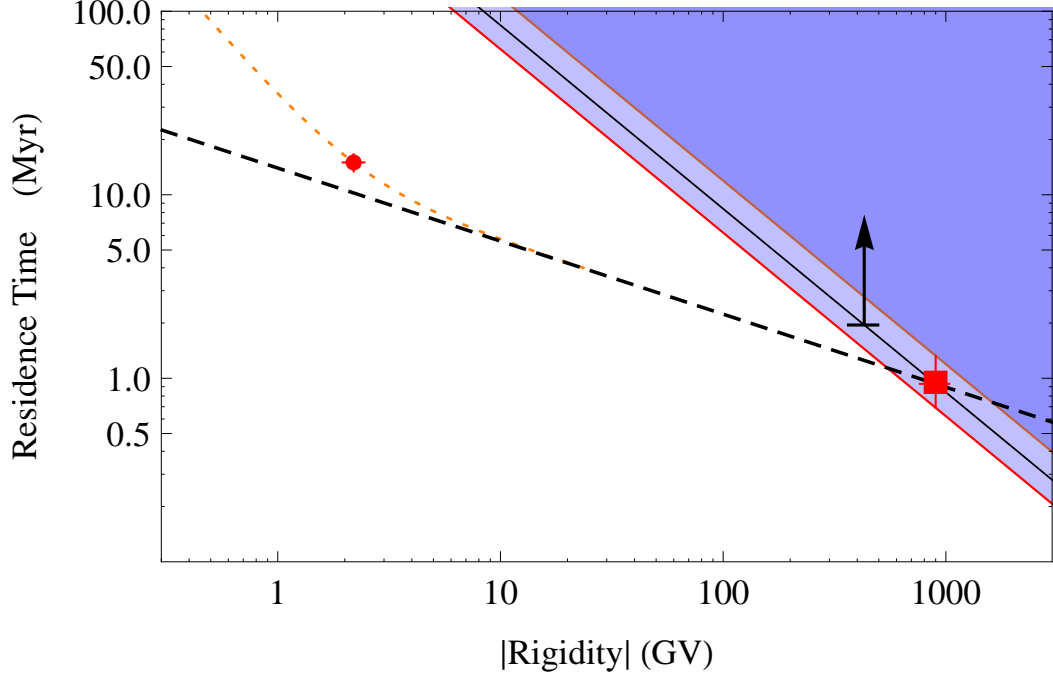


FIG. 9: Constraints on the residence time of cosmic rays in the Galaxy. The solid lines are lower limits on T_{res} obtained assuming that positrons with $E \lesssim 430$ GeV suffer negligible energy loss during their residence in the Galaxy. The different lines assume different confinement volumes and therefore different values for the average energy loss rate. The arrow corresponds to the highest energy for which a measurement of the e^+ flux is available. The point at low rigidity is the estimate on the confinement time $T_{\text{res}} = 15.0 \pm 1.6$ Myr obtained by the CRIS collaboration [31] interpreting their measurement of the $^{10}\text{Be}/^9\text{Be}$ ratio. The point at rigidity 900 GeV is estimated assuming that the break observed by HESS in the $(e^+ + e^-)$ spectrum corresponds to the critical energy where the residence and energy loss time are equal. The dotted line that connects the two points is given by expression (28) with the parameters $T_0 \simeq 14.0 \pm 0.4$ Myr and $\delta \simeq 0.40 \pm 0.04$.